

Comparing agriculture-related characteristics of flash and normal drought reveals heterogeneous crop response

Sarah Quynh-Giang Ho¹, Allan Buras², and Ye Tuo³

¹Karlsruhe Institute of Technology

²Technical University of Munich

³Chair of Hydrology and River Basin Management, Technical University of Munich

April 16, 2023

Abstract

Despite rapid progress in the burgeoning field of flash drought research, few studies directly compare the differences in characteristics between flash drought (commonly understood as quick, rapid-onset drought) and drought traditionally defined as slow-moving (henceforth normal drought), particularly over agricultural regions where drought effects may be economically the most disastrous. In this study, flash and normal drought events are identified using reanalysis soil moisture in the data-rich agricultural region of the California Central Valley for investigation of characteristics related to agriculture. In particular, we investigate the relative duration of pixels in drought events, the correlation of drought intensity with vegetation condition, the impact of aridity on vegetation response and drought, and the differences in the different characteristics between rainfed and irrigated agriculture. Overall, we found considerable differences between flash and normal drought, particularly in their spatial distributions and behavior in relation to aridity. Flash droughts even indicate a counterintuitive improvement in vegetation condition in the northern, more humid regions, likely due to the release of growth limiting factors (e.g. below-optimum temperature and radiation) associated with drought. Results also indicate improvements in vegetation conditions during normal drought for irrigated land over rainfed, highlighting the importance of irrigation as a drought protection strategy in agriculture.

Hosted file

959804_0_art_file_10852179_rsdymf.docx available at <https://authorea.com/users/603736/articles/633944-comparing-agriculture-related-characteristics-of-flash-and-normal-drought-reveals-heterogeneous-crop-response>

Hosted file

959804_0_supp_10852180_rsdmm5.docx available at <https://authorea.com/users/603736/articles/633944-comparing-agriculture-related-characteristics-of-flash-and-normal-drought-reveals-heterogeneous-crop-response>

Hosted file

959804_0_supp_10852181_rs9114.docx available at <https://authorea.com/users/603736/articles/633944-comparing-agriculture-related-characteristics-of-flash-and-normal-drought-reveals-heterogeneous-crop-response>

1 **Comparing agriculture-related characteristics of flash and normal drought reveals**
2 **heterogeneous crop response**

3 **Sarah Ho^{1,2}, Allan Buras³, Ye Tuo¹**

4 ¹ Technical University of Munich, School of Engineering and Design, Chair of Hydrology and
5 River Basin Management.

6 ² Karlsruhe Institute for Technology, Institute of Water and River Basin Management -
7 Hydrology.

8 ³Technical University of Munich, School of Life Sciences, Professorship for Land Surface-
9 Atmosphere Interactions.

10 **Key Points:**

- 11 • Flash droughts exhibit significantly different spatial distributions and trends in
12 characteristics than normal droughts
- 13 • Aridity can provide useful clues about vegetation condition and irrigation's effectiveness
14 during drought
- 15 • Flash drought conditions (temperature, radiation) may alleviate plant growth limitations
16 in cooler climates, improving vegetation condition

17

18 **Abstract**

19 Despite rapid progress in the burgeoning field of flash drought research, few studies directly
20 compare the differences in characteristics between flash drought (commonly understood as
21 quick, rapid-onset drought) and drought traditionally defined as slow-moving (henceforth normal
22 drought), particularly over agricultural regions where drought effects may be economically the
23 most disastrous. In this study, flash and normal drought events are identified using reanalysis soil
24 moisture in the data-rich agricultural region of the California Central Valley for investigation of
25 characteristics related to agriculture. In particular, we investigate the relative duration of pixels
26 in drought events, the correlation of drought intensity with vegetation condition, the impact of
27 aridity on vegetation response and drought, and the differences in the different characteristics
28 between rainfed and irrigated agriculture. Overall, we found considerable differences between
29 flash and normal drought, particularly in their spatial distributions and behavior in relation to
30 aridity. Flash droughts even indicate a counterintuitive improvement in vegetation condition in
31 the northern, more humid regions, likely due to the release of growth limiting factors (e.g.
32 below-optimum temperature and radiation) associated with drought. Results also indicate
33 improvements in vegetation conditions during normal drought for irrigated land over rainfed,
34 highlighting the importance of irrigation as a drought protection strategy in agriculture.

35 **Plain Language Summary**

36 Flash droughts are droughts that, in contrast to traditionally understood droughts, develop
37 suddenly and rapidly. This can be particularly dangerous for agriculture, since crops can be
38 affected by sudden changes in plant available water. This study identifies differences in drought
39 characteristics over the Central Valley agricultural region of California, such as length of time in
40 drought and effects on vegetation, with considerations for local climate and irrigation. Overall,
41 flash drought shows clear spatial trends that vary with local climate, with some regions showing
42 a benefit to plant health during flash droughts, and irrigated regions performing slightly better.
43 This highlights the importance of irrigation as an adaptation strategy against drought.

44 **1 Introduction**

45 Within the widely recognized phenomenon of drought is the recently recognized phenomenon of
46 flash drought. This term describes a rare but increasingly common subset of drought on a sub-

47 seasonal (weeks to months) scale (Otkin et al., 2018; Pendergrass et al., 2020). While traditional
48 drought has typically been defined by rainfall deficits, many approaches to identifying flash
49 drought are based on changes in evapotranspiration (ET) and soil moisture (Chen et al., 2019; Li
50 et al., 2020; Liu et al., 2020; Nguyen et al., 2019; Otkin et al., 2018; Otkin et al., 2016; Wang &
51 Yuan, 2018; X. Xiao et al., 2019). Despite the recent uptick in research on its identification and
52 propagation, much is still unknown about flash drought.

53 The identification of flash drought events is, much like its traditional counterpart, a developing
54 field. The subjectivity of drought definitions remains a significant barrier to a universally-
55 applicable definition (Guo, Bao, Liu, et al., 2018; Guo, Bao, Ndayisaba, et al., 2018; Sheffield et
56 al., 2009; Spinoni et al., 2019; Zang et al., 2019), though some may argue that such a definition
57 is unnecessary, stressing a functional (rather than theoretical) definition (Lloyd-Hughes, 2013).
58 Functional definitions have since been postulated for flash drought, focusing on two aspects:
59 first, that there is a rapid intensification of water deficits; and second, that the deficit reaches
60 drought conditions (Otkin et al., 2018). Several methods now exist that define flash drought
61 based on soil moisture or evaporation conditions, as these have been shown to be most closely
62 linked with flash drought (Chen et al., 2019; Ford & Labosier, 2017; Ford et al., 2015).

63 In their review of flash drought literature, Otkin et al. (2018) called for researchers to unite under
64 a singular definition of flash drought as a subset of drought characterized by a high rate of
65 intensification rather than a short duration. Such definitions can be expressed in a rate-of-change
66 relationship involving a change in severity over time. An example is that of Chen et al. (2019),
67 where flash droughts are explicitly defined by areas that, in a four-week period, experience a
68 two-category change in dryness in the U.S. Drought Monitor. Pendergrass et al. (2020) refine
69 this definition by imposing criteria that the two-category change must happen over the course of
70 two weeks and maintain that change for another two. They also propose a definition for
71 international usage based on a 50% increase in the evaporative demand drought index (EDDI)
72 over two weeks and sustained for another two. Similar intensification approaches in soil moisture
73 are used by Liu et al. (2020). However, many of these definitions are constrained to a single area
74 and may not be able to capture how drought moves and expands over time. Li et al. (2020)'s use
75 rate-of-change principles created criteria that account for both intensity and area, but also still
76 employed a short duration filter. This allows identification of flash drought with potential for

77 global use that includes their movement in space and time, which is useful for analyzing flash
78 drought and its effects over different land and vegetation types.

79 A particular concern for flash drought is its effect on agriculture. Remote sensing products,
80 particularly the Normalized Difference Vegetation Index (NDVI), have been commonly used in
81 drought monitoring as a proxy for plant health (Dong et al., 2019; Gillespie et al., 2018;
82 Goldberg et al., 2010; Gu et al., 2007; Ji & Peters, 2003). The impacts of drought on vegetation
83 have been shown to be related to local dryness, also known as aridity. While similar to drought
84 in that they both express dryness, aridity is a descriptor of conditions without reference to typical
85 levels—a key component of drought (Le Houerou, 1996) —and is typically calculated over
86 longer periods of time (Zomer & Trabucco, 2022). Orth et al. (2020) found that vegetation health
87 indicators vary with aridity—in particular, that arid regions show strong responses and humid
88 regions show weak ones—and that they intensify with increasing drought duration. This is
89 consistent with Vicente-Serrano et al. (2013), who found that regions with different aridity tend
90 to respond to drought at different time scales, with arid regions responding faster than humid
91 ones. They also hypothesize that this may be due, in part, to differing adaptation strategies in
92 local plants, which is corroborated by Buras et al. (2020). A potential explanation for this
93 behavior is that, despite a large relative anomaly suggested by standardized indicators, actual
94 water deficit conditions may not be severe enough to result in actual damage, particularly in
95 typically cool and moist regions (Zang et al., 2019). However, whether these patterns of
96 vegetation response based on aridity and duration still hold in significantly shorter flash drought
97 events has not yet been investigated.

98 As extreme events become more frequent due to changing climate, it becomes critical to
99 investigate flash drought and its effects on agriculture and food production. A frequency study of
100 flash drought over the conterminous U.S. found that, although the drought-stricken state of
101 California experiences fewer flash droughts than the rest of the country, the Central Valley
102 region—an agricultural powerhouse—still experiences extreme flash drought approximately
103 every five to six years (X. Xiao et al., 2019). Given the strong dependence on groundwater
104 withdrawal for irrigation in the region threatening local aquifers (Cody et al., 2015; Pauloo et al.,
105 2020; Wilson et al., 2016; M. Xiao et al., 2017), the degree of impact that irrigation has in
106 tempering adverse drought effects—particularly in flash drought, for which little research
107 exists—should be investigated.

108 In this study, the differences in agriculture-related characteristics of soil moisture drought—
109 namely the relationships between the NDVI-soil moisture correlation and relative duration of
110 drought—and their variations with aridity and irrigation are compared between the shorter, faster
111 onset flash drought events and normal drought events in the high-data and drought-prone region
112 of the California Central Valley. In particular, we focus on the following hypotheses (referenced
113 throughout the study as H1, H2, and H3):

- 114 • H1: Longer duration of normal drought will result in more spatially homogeneous
115 drought characteristics and more negative impacts on vegetation in comparison to flash
116 drought. As a corollary, regions spending relatively longer time per event in a particular
117 drought type will experience stronger changes in vegetation response.
- 118 • H2: The aridity of a region strongly impacts the agricultural vegetation response of a
119 region to drought. More specifically, agriculture in humid regions may benefit short-term
120 from flash drought events because the anomaly indicated by a standardized index does
121 not correspond to a true plant water deficit.
- 122 • H3: Irrigation will provide a tempering effect on adverse vegetation responses to both
123 flash and normal drought, independent of aridity.

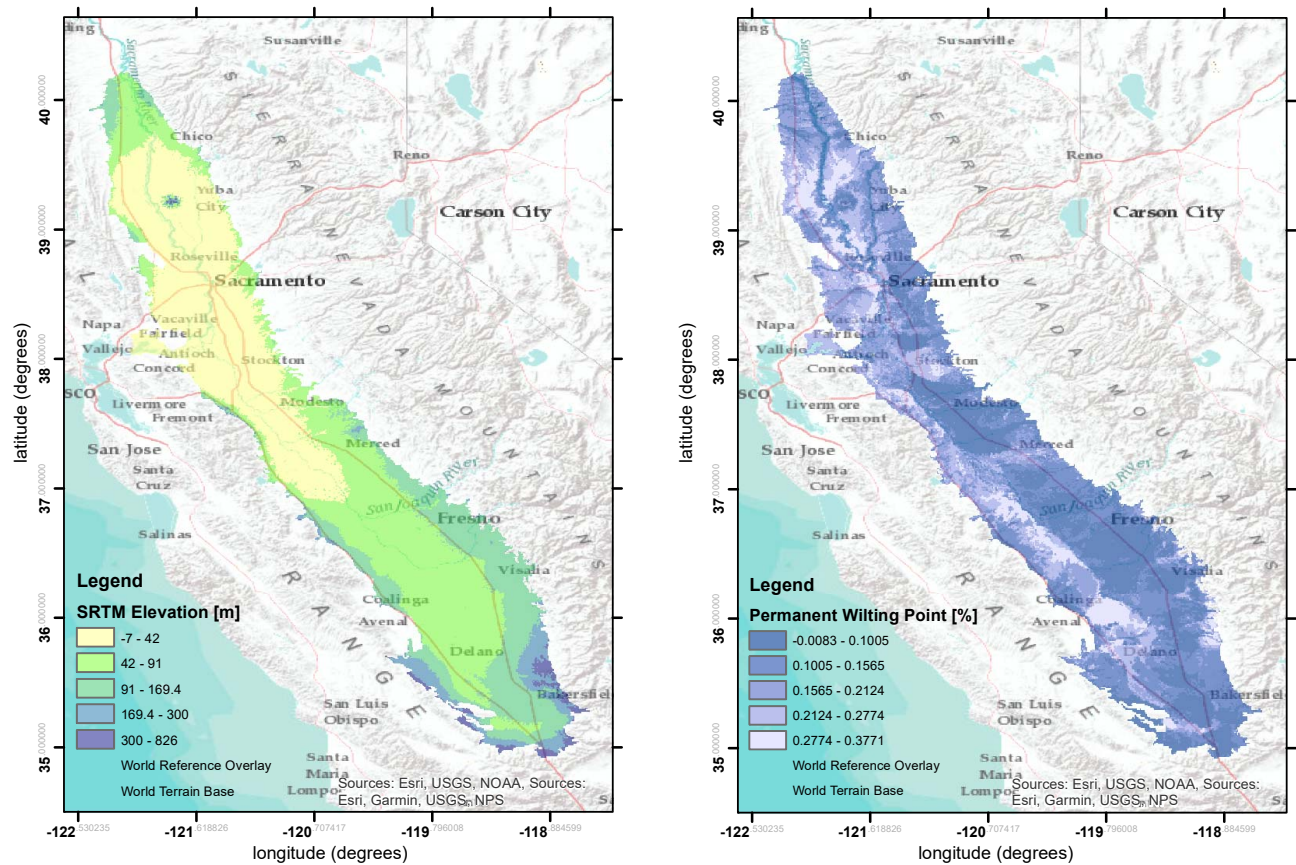
124 **2 Study Area**

125 The California Central Valley is a level three ecoregion as defined by the United States
126 Environmental Protection Agency (Griffith et al., 2016) encompassing approximately 47,000
127 km², or roughly 10% of the state's total area (Figure 1). It is a stretch of flat plains bordered by
128 coastal mountains to the west and the Sierra Nevada mountain range to the east. More than half
129 of the ecoregion is classified as farmland, which is farmed intensively throughout the year
130 (Griffith et al., 2016; Teluguntla et al., 2015). The mild climate, along with loamy soils with low
131 wilting points favorable for agriculture (Walkinshaw et al., 2022), makes it one of the largest,
132 most productive agricultural region in the United States with exports all over the world (Marston
133 & Konar, 2017).

134 However, the region—as with much of the state—is subject to frequent and intense droughts. It
135 exists in a climatic transition zone (Dong et al., 2019): while overall the region is semiarid and
136 heavily dependent on irrigation, particularly groundwater (Cody et al., 2015), the northern half of
137 the area is generally cooler and wetter than the southern part. Several studies have indicated a

138 drying trend in California, particularly in the southern region (Dong et al., 2019; Okin et al.,
139 2018).

140 The recent 2011-2017 drought that peaked in 2013 is considered among the most intense and
141 severe in recent history (Dong et al., 2019; Erlingis et al., 2021; Griffin & Anchukaitis, 2014;
142 Lund et al., 2018; M. Xiao et al., 2017), resulting in heavy aquifer withdrawals that resulted in
143 soil subsidence (Cody et al., 2015; M. Xiao et al., 2017). To avoid the significant skew this
144 historic drought will add to the data, this study will focus on available data through 2012.



145
146

147 Figure 1. Elevation map (left) of the study area (California Central Valley, USEPA Ecoregion 7),
148 generated using SRTM (NASA-JPL, 2013), and permanent wilting point (PWP) as volumetric soil water
149 content (right), calculated using soil data from Walkinshaw et al. (2022) according to Saxton and Rawls
150 (2006). Negative values in PWP are likely due to errors in the data source, as it is meant to depict trends
151 in soil properties and not necessarily the exact conditions.

152 3 Data and Methods

153 3.1 Drought and Flash Drought Identification

154 This work applies the methodology of Li et al. (2020) for identifying and tracking flash droughts
 155 for the study area of the California Central Valley with some slight modifications. Though the
 156 originally developed for use with the Standardized Evaporative Deficit Index (Vicente-Serrano et
 157 al., 2018), the method should be applicable with any standardized index (SI). In brief, the method
 158 (with modifications) is as follows (Li et al., 2020):

- 159 1. *Identification of drought patches (clusters)* above an area threshold using a chosen
 160 drought index calculated on a five-day timescale. In this study, the area threshold is 1.6%
 161 of the study area (roughly 750 km²), and the drought index used is the Standardized Soil
 162 Moisture Index (SSmI) (AghaKouchak, 2014; Hao & AghaKouchak, 2013) calculated on
 163 a 5-day scale for every available time step. To be part of a cluster, a pixel must
 - 164 a. have an SI value of less than or equal to -1 (threshold dryness)
 - 165 b. be adjacent to another pixel with SI < -1 in the cluster
- 166 2. *Checking spatial connection of drought clusters.* The spatial connection between two
 167 clusters in consecutive timesteps is verified by the conditions that they must be
 - 168 a. more than 50% of the area of the smaller drought cluster, and
 - 169 b. more than the minimum drought cluster area threshold (1.6% of the study area).
- 170 3. *Elimination of connected clusters lasting less than a total of five pentads (25 days).* In
 171 this work, all remaining collections of clusters after this step are considered drought
 172 events. Subsequent steps are used to differentiate flash droughts from normal droughts.
- 173 4. *Division of the event into development and recovery phases.* This is done using the rate of
 174 change of the drought intensity of the whole patch (drought patch intensity DPI), for each
 175 time step k

$$DPI_k = \sum_{i=1}^n SI \quad (1)$$

176 where SI is the value of the standardized drought index (in this case SSmI) for a
 177 particular point and n is the number of points in the drought patch. The timestep with the

178 most negative value of DPI is considered the peak intensity; all timesteps before the peak
179 are the development period and all timesteps after are the recovery period.

180 5. *Calculation of the instantaneous intensification rate (IIR) and the average IIR (AIIR).*
181 The IIR is based on the change of DPI, referred to as the cumulative standardized value
182 (CSV):

$$CSV_k = DPI_{k+1} - DPI_k \quad (2)$$

183 The change in CSV for each time step, adjusted for grid size by dividing by the total
184 number of pixels n involved in each drought patch, is calculated as

$$\Delta \overline{CSV}_{k,k+1} = \frac{CSV_{k+1} - CSV_k}{n_{k,k+1}} \quad (3)$$

185 The IIR is then the division of the change in CSV by the difference in time steps t :

$$\begin{aligned} IIR_{k,k+1} &= \frac{\Delta \overline{CSV}_{k,k+1}}{t_{k+1} - t_k} \\ &= \frac{1}{t_{k+1} - t_k} \left(\frac{DPI_{k+2} - 2 DPI_{k+1} + DPI_k}{n_{k,k+1}} \right) \left(\frac{DPI_{k+2} - 2 DPI_{k+1} + DPI_k}{n_{k,k+1}} \right) \end{aligned} \quad (4)$$

186 Given this forward calculation, it follows that the calculation of IIR—and by extension,
187 AIIR—is only possible for $m - 2$ timesteps, where m is the total number of timesteps in
188 the drought event. Thus, the average IIR (AIIR) is calculated as the average values of the
189 IIR for $m - 2$ timesteps during the flash drought development period (i.e. until the peak of
190 drought) only,

$$AIIR = \frac{\sum_{i=1}^{m-2} IIR_{k,k+1}}{m} \quad (5)$$

191 It should be noted that these equations here assume intensification, i.e., that IIR and AIIR
192 will be negative. If they are positive, this indicates a recovery rate, and are identified by
193 Li et al. (2020) as an instantaneous recovery rate (IRR) and average IRR (AIRR).

194 6. *Identification of flash drought events.* To be considered a flash drought event, the event
195 must fulfill all the following criteria:

196 a. The duration of the event lasts longer than five pentads (25 days);

- 197 b. The duration of the event may not exceed twelve pentads (60 days); and
 198 c. The AIIR is more negative than or equal to the 45th percentile of the cumulative
 199 distribution frequency of $\Delta\overline{CSV}$ during the development phase.

200 Drought events that satisfy *a* but fail *b* and / or *c* are considered traditional or normal
 201 drought events.

202 An additional criterion in the original study proposed that one or more IIR should exist that are
 203 less than or equal to the 25th percentile of the cumulative distribution frequency of $\Delta\overline{CSV}$ during
 204 the development phase; however, because this study uses a daily timestep, the $\Delta\overline{CSV}$ and IIR are
 205 equivalent:

$$IIR_{k,k+1} = \frac{\Delta\overline{CSV}_{k,k+1}}{t_{k+1} - t_k} = \frac{\Delta\overline{CSV}_{k,k+1}}{1} = \Delta\overline{CSV}_{k,k+1} \quad (6)$$

206 Thus, the additional criterion is superfluous and has been omitted.

207 It is important to note that this definition of flash drought is significantly more stringent on
 208 duration than most contemporary definitions. Whereas most definitions require an end in drought
 209 conditions within a designated development period (for which the consensus, according to
 210 Lisonbee et al. (2021), is within 40 days), thus emphasizing a rapid onset, this definition requires
 211 that a drought event develops and terminates within 60 days. However, other aspects of this
 212 definition—namely the inclusion of area in the definition, the ability to detect smaller drought
 213 events more relevant for agricultural usage, and the ability to identify events and all pixels
 214 involved in the event at each time step—make this useful for the study of flash drought and
 215 particularly for the spatial distribution of its impacts.

216 3.2 Datasets and Drought Indices

217 3.2.1. Calculation of the Standardized Soil Moisture Index (SSmI)

218 The Standardized Soil Moisture Index (SSmI) (AghaKouchak, 2014; Hao & AghaKouchak,
 219 2013) is a drought index calculated using the same standardized method as the commonly-used
 220 Standardized Precipitation Index (SPI) (McKee et al., 1993). The SSmI is based on the root zone
 221 soil moisture—in this study, defined as soil moisture from the top 100 cm of soil (Erlingis et al.,
 222 2021)—and exhibits high autocorrelation, indicating a heavy dependence on previous values

223 (AghaKouchak, 2014). Mild drought is defined as an SSmI of 0 to -0.99; moderate drought is -
224 1.00 to -1.49; severe drought is -1.50 to -1.99; and extreme drought is less than -2.00.

225 The Standardized Drought Analysis Toolbox (Farahmand & AghaKouchak, 2015) is a
226 generalized framework for calculating standardized drought indices. A main feature of this
227 toolbox is that it eliminates the need for fitting distribution curves to the data, a challenge that
228 can hinder the comparability of different standardized indices across variables (Bayissa et al.,
229 2018; Farahmand & AghaKouchak, 2015; Hao & AghaKouchak, 2013; Stagge et al., 2015), by
230 using the Gringorten empirical plotting position (Gringorten, 1963) rather than probability
231 distribution curves to calculate the probability of occurrence. This study uses the modified SDAT
232 method used in Ho et al. (2021) to calculate the SSmI on a five-day, rather than 30-day,
233 timescale. This modified method also includes the Weibull non-exceedance probability to deal
234 with zero-data occurrences per Stagge et al. (2015) and uses a daily, rather than a monthly, time
235 step to generate a daily-time-step dataset.

236 Components for calculating the root zone soil moisture were taken from the Western Land Data
237 Assimilation System (WLDAS), a recently released fine-scale ($0.01^\circ \times 0.01^\circ$), daily land surface
238 model based on remote sensing data developed for the study of near-surface hydrology.
239 Meteorological forcing drives a land surface model containing leaf area index, vegetation class
240 and soil texture to simulate energy and water budget processes. As a collaborative effort between
241 the National Aeronautics and Space Administration (NASA) and the California State Water
242 Resources Control Board (SWRCB) (Erlingis et al., 2021), it is a special instance of NASA's
243 Land Data Assimilation System (LDAS) that is customized for the Western United States for the
244 purpose of sustainable groundwater planning in California (Erlingis et al., 2021). Root zone soil
245 moisture was calculated as the sum of volumetric soil moisture in the top three layers of soil
246 (total depth of 100 cm) and does not include additional input from irrigation.

247 3.2.2. Calculation of the NDVI z-Score (zNDVI)

248 The Normalized Difference Vegetation Index (NDVI) is a measure of vegetation greenness from
249 the combination of the red and near-infrared bands collected by satellite data, calculated as

$$NDVI = \frac{\rho_{NIR} - \rho_R}{\rho_{NIR} + \rho_R} \quad (7)$$

250 where the red bands indicate absorption by plant chlorophyll during photosynthesis and the near-
 251 infrared bands are affected by leaf structure. The NDVI ranges from 0 to 1, with 1 being the ideal
 252 value (Goldberg et al., 2010; Tucker, 1979). Key weaknesses of the NDVI include its sensitivity
 253 to soil brightness and color, atmospheric interference, and sensor calibration (Huang et al., 2020;
 254 Xue & Su, 2017). Despite the existence of other similar indices that improve on these, the NDVI
 255 remains widely popular due to its ease of calculation and abundance of available data
 256 (AghaKouchak et al., 2015; Huang et al., 2020; Xue & Su, 2017). Studies using the NDVI and
 257 its derived products have indicated that even short dry spells can have damaging effects on crop
 258 health and production (Ji & Peters, 2003; Nicolai-Shaw et al., 2017; Orth & Destouni, 2018;
 259 Otkin et al., 2016; Vicente-Serrano et al., 2013), with some suggesting that certain vegetation
 260 types can attenuate drought effects (Pendergrass et al., 2020).

261 This study uses data from the Moderate Resolution Imaging Spectrometer (MODIS) (Spruce et
 262 al., 2016). It is a smoothed, gap-filled, composite dataset composed of data from both the Terra
 263 and Aqua satellites. The satellites collected on an 8-day time step for the conterminous United
 264 States from January 1, 2000, through December 31, 2015 (Spruce et al., 2016). Per year, there
 265 are 46 timesteps each representing 8 days (for the 46th timestep of the year, the first values of the
 266 next year are included). It was upscaled to the WLDAS grid using the weighted average method.

267 Because the NDVI value is a measurement for the period without historical context, further
 268 processing is needed to be able to compare it with drought indices (Huang et al., 2020; J. Peng et
 269 al., 2020; Peters et al., 2002). For this study, NDVI is prepared for comparison with drought
 270 indices by calculating the z-score of the observation in the style of Peters et al. (2002), where the
 271 z-score for a coordinate i for timestep j of 46 in year k can be calculated as

$$zNDVI_{ijk} = \frac{NDVI_{ijk} - \overline{NDVI}_{ij}}{\sigma_{ij}} \quad (8)$$

272 where \overline{NDVI}_{ij} is the average NDVI for the given pixel at the given timestep across the entire
 273 observed period, and σ_{ij} is the standard deviation for the same pixel at the same timestep.

274 The z-score can be understood as the number of standard deviations an observed value is from
 275 the mean—in other words, the degree of abnormality. The z-score has been used for comparison
 276 of NDVI with other drought indices in several studies (Dong et al., 2019; J. Peng et al., 2020;

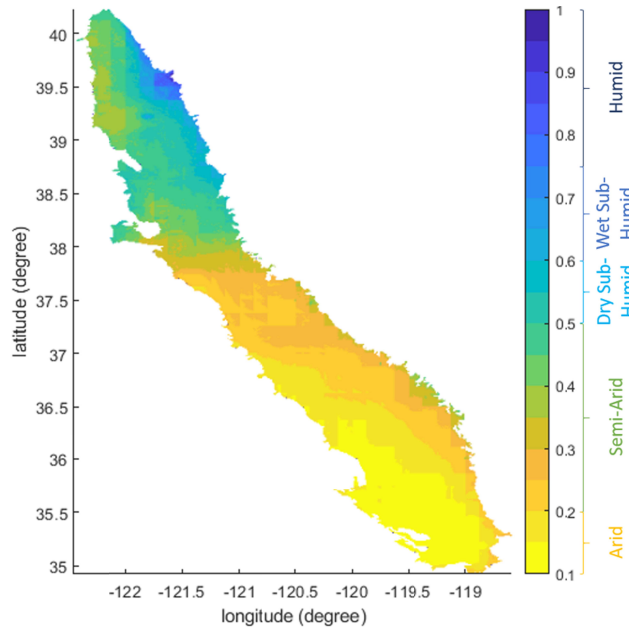
277 Peters et al., 2002), though it should be noted that such comparisons are best limited to trend
278 analysis due to the different calculation methods.

279 3.2.3. Division of Irrigated Agriculture using the Global Food Security Analysis and Data
280 (GFSAD)

281 The Global Food Security Analysis and Data (GFSAD) 1 km crop extent dataset (Teluguntla et
282 al., 2015), masked to the study area, assigns irrigation status (watering method) to each pixel in
283 the area. Major irrigation, minor irrigation, and rainfed pixels consist of more than 50% (by area)
284 cropland and are differentiated by how the cropland is irrigated (Teluguntla et al., 2015).
285 Irrigation in this dataset is explicitly defined as the “artificial application of any amount of water
286 to overcome water stress” (Teluguntla et al., 2015), including land that is irrigated only once;
287 rainfed areas are land that receives no additional water to overcome water stress. Major and
288 minor irrigation differ not in the amount of water added, but rather the source of the water for
289 irrigation (Teluguntla et al., 2015). Though in many places the distinction between major and
290 minor irrigation can be difficult to parse, Teluguntla et al. (2015) explicitly name the CA Central
291 Valley as a location where they are clearly distinguished. The decision to exclude minor
292 irrigation, rather than lump it with major irrigation, is because minor irrigation sources are more
293 likely to be privately owned and can be drawn with relatively fewer restrictions, making it more
294 difficult to regulate. This study therefore only focuses on major irrigated—henceforth irrigated—
295 agriculture (19% of study area) and rainfed agriculture (42.2% of study area).

296

3.2.4. Aridity



297

298 Figure 2. The aridity index (ratio of total precipitation to total potential evapotranspiration) for the study
 299 area.

300 An aridity index (Le Houerou, 1996) was calculated to characterize the water-energy relationship
 301 of the study area (Figure 2), where aridity is the ratio of energy to available water:

$$Aridity = \frac{\sum Precipitation}{\sum Potential ET} \quad (9)$$

302 A smaller aridity index indicates that there is more energy than water and therefore more arid; a
 303 larger aridity index indicates more water and therefore more humid. Potential ET was calculated
 304 using the FAO-56 Penman Monteith method (Zotarelli et al., 2010) with components from
 305 WLDAS and the SRTM Digital Elevation Model (NASA-JPL, 2013). More than half of the
 306 region (55.92%) is classified as semiarid (aridity of 0.2-0.5), less than half (31.32%) is classified
 307 as arid (aridity of 0-0.2), 10.55% is considered dry sub-humid (aridity of 0.5-0.6), 1.43% is wet
 308 sub-humid (aridity of 0.6-0.75), and the rest (0.78%) is humid (aridity > 0.75).

309

3.3. Drought Characteristics

310 Droughts in this study are further studied using three degrees of dimensionality: by drought type
 311 (flash or normal drought); by drought severity class (moderate, severe, extreme, or a combination

312 of all severities above the threshold dryness described in 3.2.1); and by irrigation method as
 313 defined by the GFSAD dataset (major irrigation and rainfed) (Teluguntla et al., 2015).

314 The analysis of drought events requires the refining of the datasets to relevant events. For each
 315 drought event identified using the drought identification method described in section 3.1, an
 316 event time series is generated via a collection of the SSMI time series for every pixel in the event
 317 for the entire drought duration, regardless of how long the pixel is involved. This process is
 318 repeated for all drought events to ensure that analyses are conducted for drought events only.

319 3.3.1. Average Relative Drought Duration (ARDD)

320 Drought events, particularly normal droughts as defined in the method described in 3.1, can vary
 321 greatly in duration. Moreover, the flexible spatial and temporal definitions of the method allow
 322 situations where a pixel may only spend one or two time steps in a drought event. This makes it
 323 difficult to compare effects of duration between different events, particularly between flash and
 324 normal droughts. Here, we propose an average relative drought duration (ARDD) as a metric to
 325 generalize duration over multiple events for investigating the corollary to H1.

326 The relative drought duration (RDD) is a characteristic that expresses how long a pixel is
 327 involved in a drought event relative to the total drought duration. It can be considered a measure
 328 of a pixel's persistence or prominence in a drought event. The relative duration for a pixel i in a
 329 single drought event is calculated as the fraction

$$RDD_i = \frac{t_i}{t} \quad (10)$$

330 where t_i is the total number of time steps spent in drought and t is the total duration of the
 331 drought event. The average relative drought duration (ARDD) is then calculated across all
 332 drought events n in which the pixel exists:

$$ARDD_i = \frac{\sum_1^n RDD_i}{n} \quad (11)$$

333 If a positive relationship between ARDD and vegetation response can be established (corollary
 334 to H1), a higher ARDD can indicate that a pixel is more likely to suffer from long-term drought
 335 effects.

336 3.3.2. Correlation to zNDVI

337 Calculation of the Pearson correlation coefficient r is commonly used to determine the strength
338 of relationship between two variables, with 1.0 being the highest possible correlation, -1.0 being
339 the highest possible anticorrelation, and 0 indicating no relation (Taylor, 1990). Such
340 information is useful for determining the effects of drought on vegetation health: because the
341 correlations are calculated exclusively during drought events (i.e. when SSmI values are
342 negative), a positive correlation during a drought event would indicate a deterioration of
343 vegetation health, while a negative correlation would indicate improved conditions despite
344 drought conditions. Only statistically significant ($p < 0.05$) correlations between zNDVI and the
345 SSmI (calculated during all drought events between 1 Jan 2000 – 31 Dec 2012) were considered.
346 This zNDVI-SSmI correlation will be the key metric in investigating drought impacts on
347 vegetation (H1, H2, H3).

348 Since the zNDVI has values on an 8-day return period, while SSmI has daily-scale values, an
349 additional 8-day time series for the SSmI was generated by selecting every eighth value to
350 correspond with the zNDVI. Thus, each year has 46 values for SSmI, and zNDVI, with the 46th
351 value extending into the beginning of the next year.

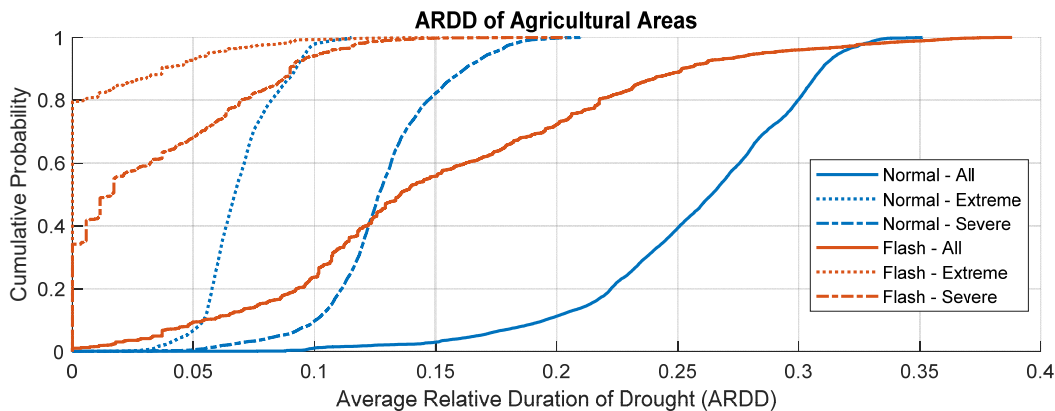
352 4 Results & Discussion

353 4.1. Identified Drought Events

354 41 drought events were identified using the method in 3.1 (34 normal drought and 7 flash
355 drought; for the complete list of events, see S1). In general, the duration of observed droughts
356 ranges from the minimum length for a drought event (25 days) to 254 days while droughts
357 occurred up to more than once per year. Flash droughts occurred at an average frequency of once
358 every five years, which is in agreement with X. Xiao et al. (2019). No flash droughts were
359 identified using the method in the 1990's, despite dry conditions. Comparison with the United
360 States Drought Monitor (Svoboda et al., 2002) show that the method is generally in agreement
361 with rapid increases in USDM-categorized area (S2).

362 4.2. Average Relative Drought Duration (ARDD)

363 Cumulative distribution functions of time spent in drought (ARDD) are plotted for both drought
 364 types (Figure 3). Additional categorical divisions are made for severe and extreme drought
 365 conditions. The shape of the curves indicate that pixels in normal drought not only spend
 366 relatively more time in drought conditions but are also less statistically variable (H1).



367

368 Figure 3. Cumulative distribution functions for relative drought duration of pixels under normal and flash
 369 drought. Additional lines indicate ARDD of severe (dotted) and extreme (dashed) conditions during the
 370 respective drought events.

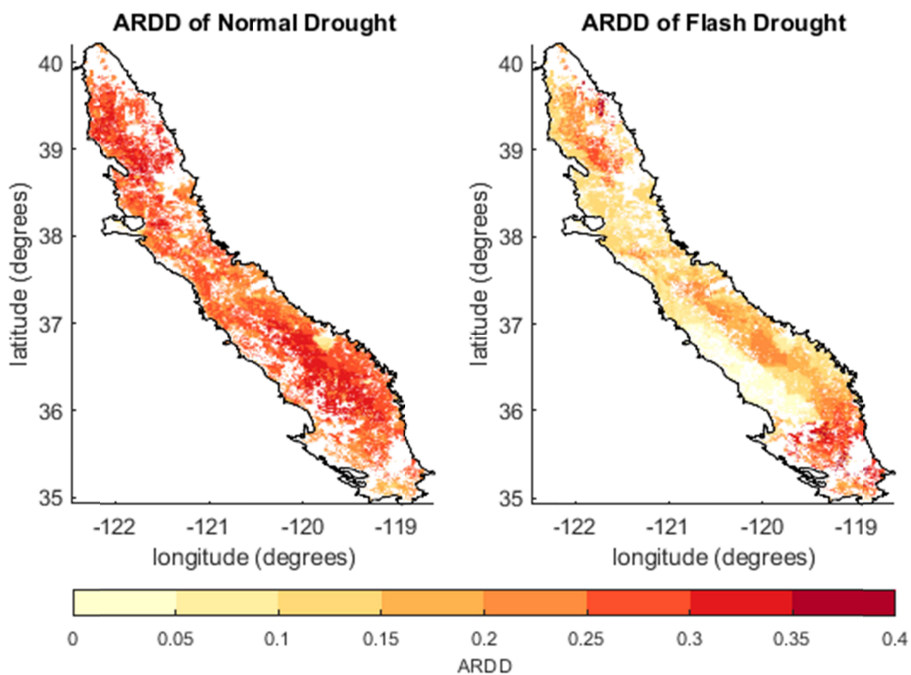
371 For normal drought events, relative duration information should be viewed with caution, as these
 372 cover a broad range of durations from 25 to over 200 days in length. Pixels spend 10-35% of the
 373 total duration in drought. Using this relative duration statistic for the median event (69 days), this
 374 would mean anywhere from 7 to 25 days in drought. The relative briefness in drought events,
 375 especially those in extreme and severe intensity, implies that the event has a quick and intense
 376 onset; this should not be surprising, considering that is the type of drought events that the
 377 identification method was designed to find.

378 Flash drought events show a drastically different behavior. These pixels spend up to 40% of their
 379 time in drought events. Assuming the median duration of 28 days, this means they will spend
 380 anywhere from 1 to 12 days in a drought event, with a relatively even probability distribution
 381 inferred from the curves' linearity. This is astoundingly short compared to the traditional drought
 382 events. Roughly 35% of pixels never reach severe drought conditions (this number increases to
 383 80% for extreme conditions), indicating that these have a quick onset rather than a rapid

384 intensification of drought. This is possible due to the dynamic spatial aspect of the drought
385 identification method, allowing drought clusters to “move” across the study area.

386 4.2.1. Spatial Distribution of ARDD

387 Spatial maps of the ARDD for both normal and flash drought are shown in Figure 4. Flash
388 drought shows significant spatial variability. Pixels experience relatively longer drought duration
389 in the southern and northern tips, which are the climatic extremes (driest in the south and most
390 humid in the north), and along the inland center. Shorter durations are distributed relatively
391 evenly throughout the rest of the catchment, though the southwestern edge of the catchment
392 seems to experience significantly shorter durations. The spatial patterns seem to correspond less
393 to those of aridity (Figure 2) and more to the permanent wilting point (Figure 1). This makes
394 sense, given that the events were defined by soil moisture anomalies and that different soil
395 characteristics (roughly represented by the wilting point) have different water retention
396 capacities. Different soils will therefore be more sensitive to shorter time scales. However, such
397 patterns cannot be identified in normal, longer drought. This suggests, in support of H1, that the
398 additional length of normal drought allows the ARDD to become independent of soil type and
399 thus more spatially homogeneous.



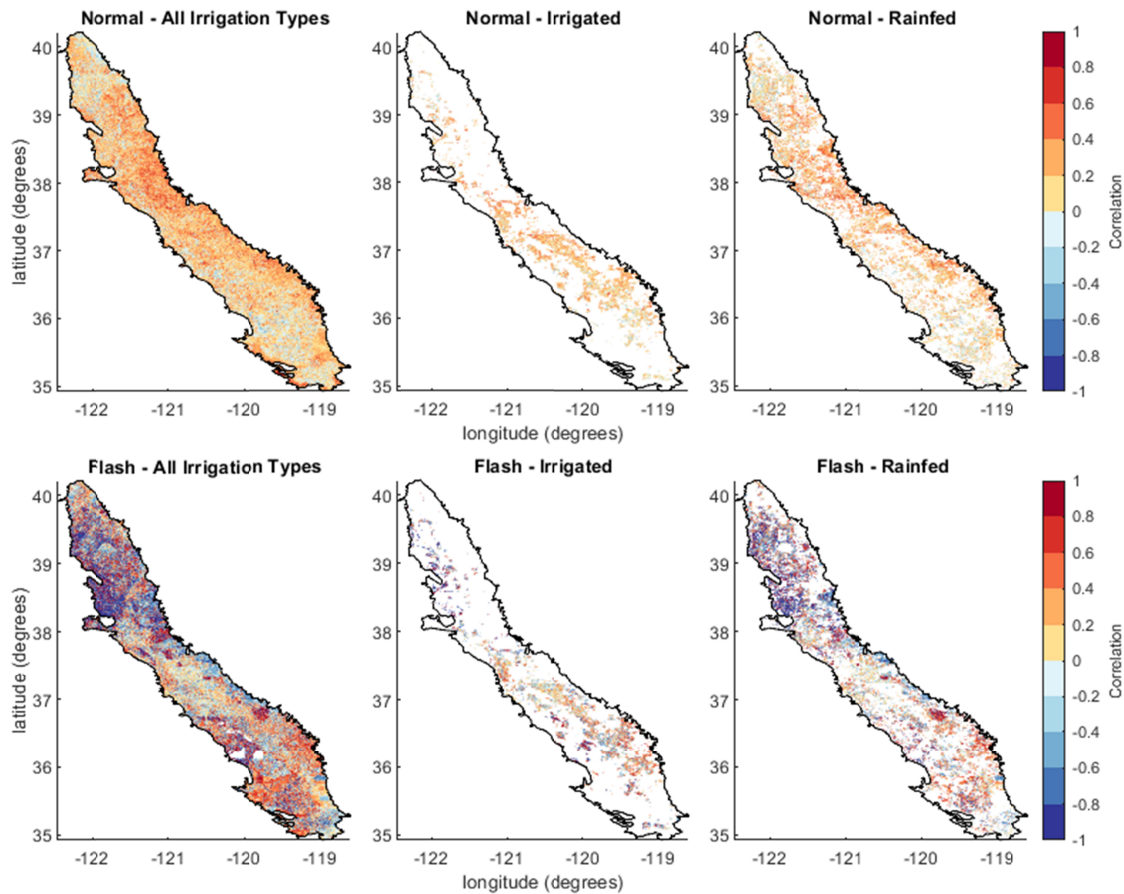
401 Figure 4. Spatial distribution of relative SSmI-defined drought duration, differentiated by normal drought
402 (left) and flash drought (right) for irrigated and rainfed pixels.

403 4.3. Correlation to zNDVI

404 Spatial maps of the zNDVI-SSmI correlation during flash and traditional drought are shown in
405 Figure 5.

406 Overall, normal drought correlations are both more negative and less spatially variable than flash
407 drought, which agrees with H1. The correlation results in normal drought show slightly more
408 positive correlations for rainfed pixels over irrigated pixels (for more, see S3), suggesting a
409 potential damping effect of irrigation (H3). This roughly corroborates the findings of Lu et al.
410 (2020): rainfed crops are more affected by drought than irrigated crops. A possible explanation
411 could be that areas with rainfed irrigation are in more humid areas with less need for additional
412 irrigation (H2); however, the lack of additional water during drought may mean crop growth will
413 be limited by water availability. The range of correlation coefficients may also be a result of
414 different crop types and timing: previous work has indicated that different crops respond faster to
415 soil moisture conditions (C. Peng et al., 2014), and that crops exhibit higher sensitivity to
416 moisture conditions in their reproductive stages, which are highly seasonal (Ji & Peters, 2003).
417 This analysis was unable to include detail on specific crops due to limitations on available crop
418 data during each drought event.

419 Correlation with SSmI during flash drought shows very strong anticorrelation in the north,
420 weaker correlations and anticorrelations in the center, and a stronger tendency towards positive
421 correlations in the south. These spatial patterns are partly mirrored by patterns of aridity (Figure
422 2), lending credence to H2. Rainfed pixels again show stronger correlation—both negative and
423 positive—to zNDVI than irrigated pixels (H3). Correlations for flash drought show visible
424 differences between irrigation types, which shows that rainfed cropland tends to be
425 anticorrelated.



426

427 Figure 5. Correlation of SSMI and zNDVI during normal and flash drought events and for different
 428 irrigation types.

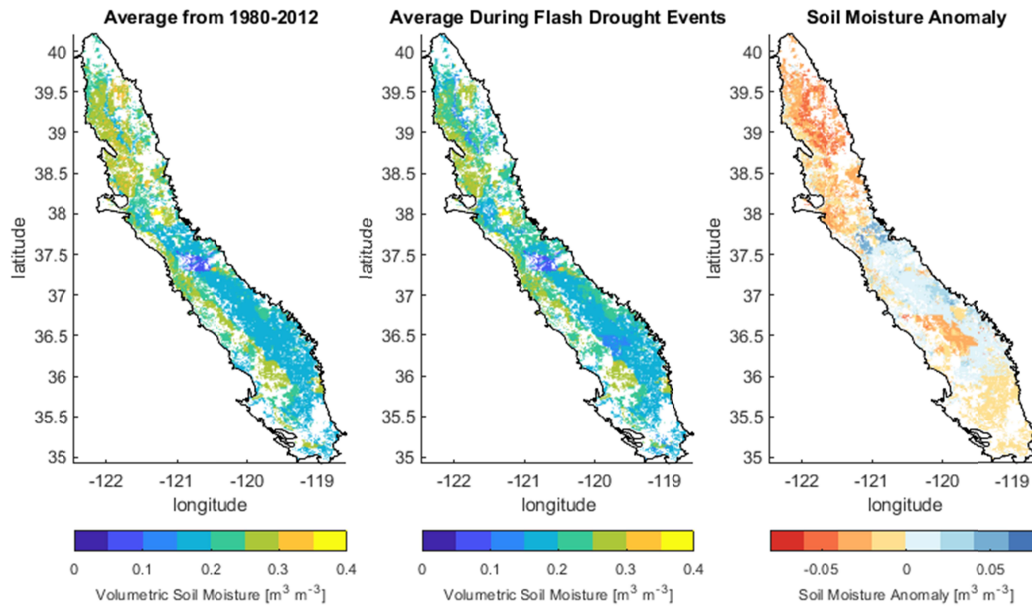
429 Such results are also consistent with previous work on the relationships between drought and
 430 agriculture. Dong et al. (2019), for example, found that during the landmark 2012-2016
 431 California drought, severe NDVI decreases accompanied drying in the southern end of the state
 432 while the northern end saw increased NDVI. They posited that the counterintuitive improvement
 433 of vegetative health in the north, despite water shortages, could be a result of warmer
 434 temperatures assisting plant growth. While the timescales of drought are vastly different, such
 435 findings are consistent with the strong anticorrelation with SSMI in the northern end—indicating
 436 an increase in NDVI despite a decrease in SSMI—and the tendency towards positive correlation
 437 in the southern end. An additional study suggests that this may also be related to the aridity of
 438 the region (Orth et al., 2020): the northern region, which is less arid, suffers significantly less
 439 from drought and can even benefit from relatively drier conditions, depending on the situation.
 440 These explanations, along with the assumption that flash droughts can be temperature driven

441 (Mo & Lettenmaier, 2015), can help explain why there are such clear differences in regions.
442 However, without investigation of the actual water supply (in this case soil moisture), a causal
443 relationship between flash drought and zNDVI cannot be established due to the potential
444 misrepresentation of actual water stress inherent in standardized indices (Zang et al., 2019). This
445 will be explored in section 4.3.1. Low SSmI values in the humid north may still indicate
446 sufficient plant available water, but may be associated with warmer temperatures and more
447 photosynthetically active radiation (Ford & Labosier, 2017). Thus, relatively drier conditions
448 could—under certain situations—stimulate plant growth.

449 A weakness of these correlation results is that these time series do not have many data points.
450 Each drought event lasts a minimum of 25 days, with flash droughts capping at 60 days. Given
451 that the NDVI dataset only collects values once every 8 days, and values are only extracted from
452 within the drought event, a flash drought event will only have at minimum 3 and at maximum 7
453 data points. Because flash drought events are few, the number of data points for correlation are
454 also few—this could mean that the correlations could change significantly as more events are
455 identified either over a larger spatial domain or with longer future records.

456 4.3.1. Soil Moisture Conditions

457 Maps describing the average volumetric soil moisture content for irrigated and rainfed cropland
458 during the entire observation period, during exclusively flash drought events, and the difference
459 between the two can be seen in Figure 6.. It should be noted that only flash droughts from the
460 NDVI observation period (2000-2012) are used here, as this investigation is intended to explore
461 the correlation results (H2) in further detail.



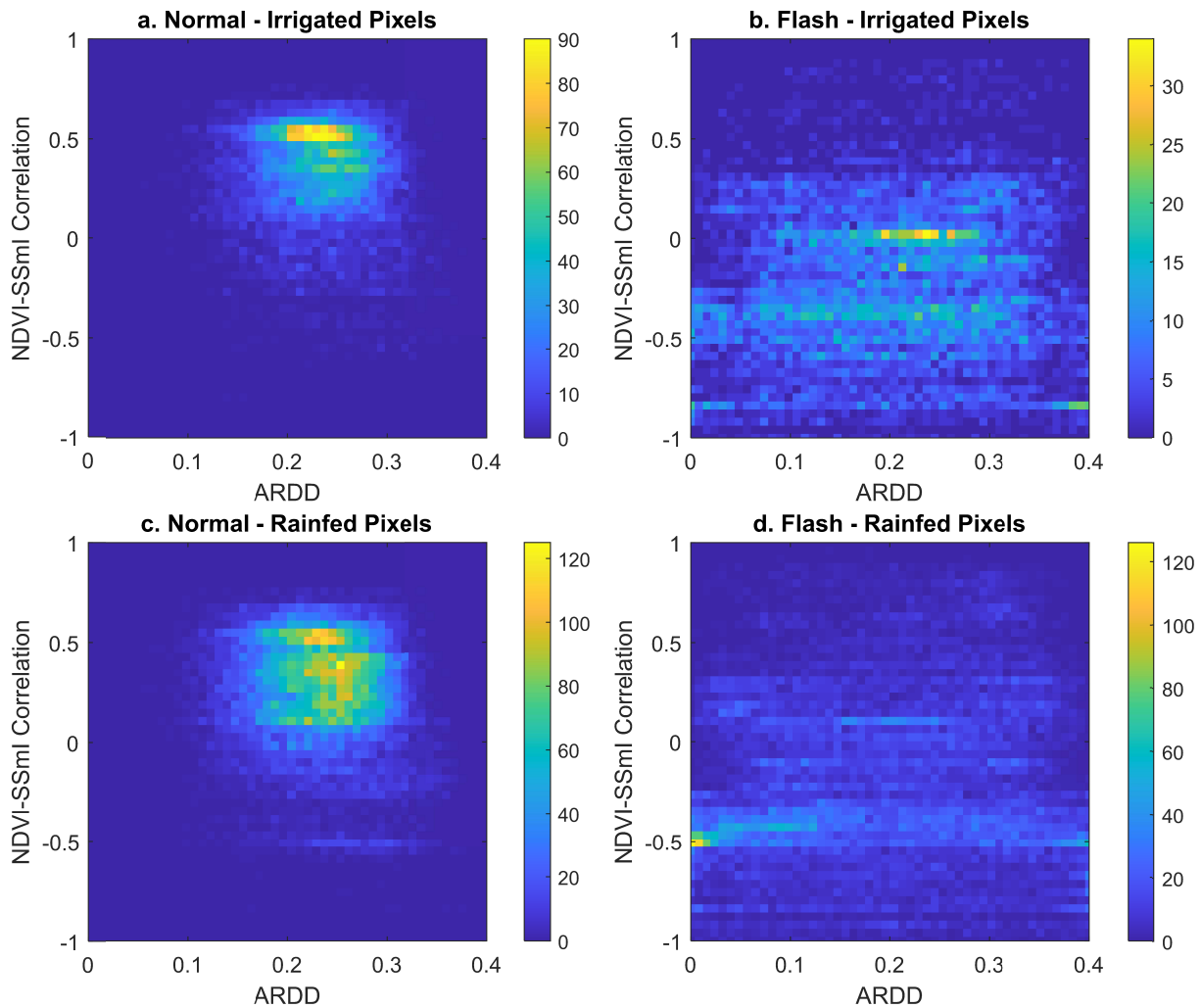
462

463 Figure 6. Maps displaying average volumetric soil moisture content [m^3/m^3] for the entire observation
 464 period (1980-2012), for exclusively flash drought durations during the NDVI observation period (2000-
 465 2012), and the anomaly. Only irrigated and rainfed cropland is shown.

466 In general, the high-anticorrelation regions in the northern section do experience a significant
 467 drop in soil moisture content under flash drought; however, the remaining soil moisture content
 468 during flash drought still generally remains close to or above 20%. While these areas do have the
 469 highest decreases in soil moisture, the remaining soil moisture is generally above the estimated
 470 permanent wilting point (Figure 1). This suggests that the average water deficit during the flash
 471 droughts in this northern region is, despite the standardized index value, not severe enough to
 472 cause permanent damage to the crops cultivated. In other words, dry soil moisture conditions
 473 (particularly if there is still plant available water) do not inherently result in plant stress, which is
 474 in agreement with H2 and with Zang et al. (2019), and may also depend on soil texture.
 475 Moreover, previous literature has suggested that there is a significant lag between water
 476 shortages and effects on NDVI that may not be captured in this short time period (C. Peng et al.,
 477 2014). These issues could be rectified in future studies by adding more time steps before and / or
 478 after the duration of the drought event to include potential lagging effects, and by extending the
 479 observed time period to include more flash drought events. However, the inclusion of the
 480 recovery phase in the drought identification method allows at least partial inclusion of any
 481 potential lag times in vegetation response in this study.

482 Interestingly, an increase in average soil moisture is seen in the central region of the study area
 483 during flash drought events—while it may seem counterintuitive, this may be attributed to the
 484 lack of seasonal context that an arithmetic mean has in comparison to the standardization process
 485 used when calculating SSmI. In other words, the soil moisture conditions during flash drought
 486 was dry for that particular day of the year, but overall higher than the arithmetic average for the
 487 total observation period (for example, a soil moisture content of $0.3 \text{ m}^3/\text{m}^{-3}$ in a historically wet
 488 month, e.g. January, could result in $\text{SSmI} = -1.5$, but the average soil moisture content over 32
 489 years could be $0.2 \text{ m}^3/\text{m}^{-3}$).

490 4.3.2. Relationship to ARDD



491

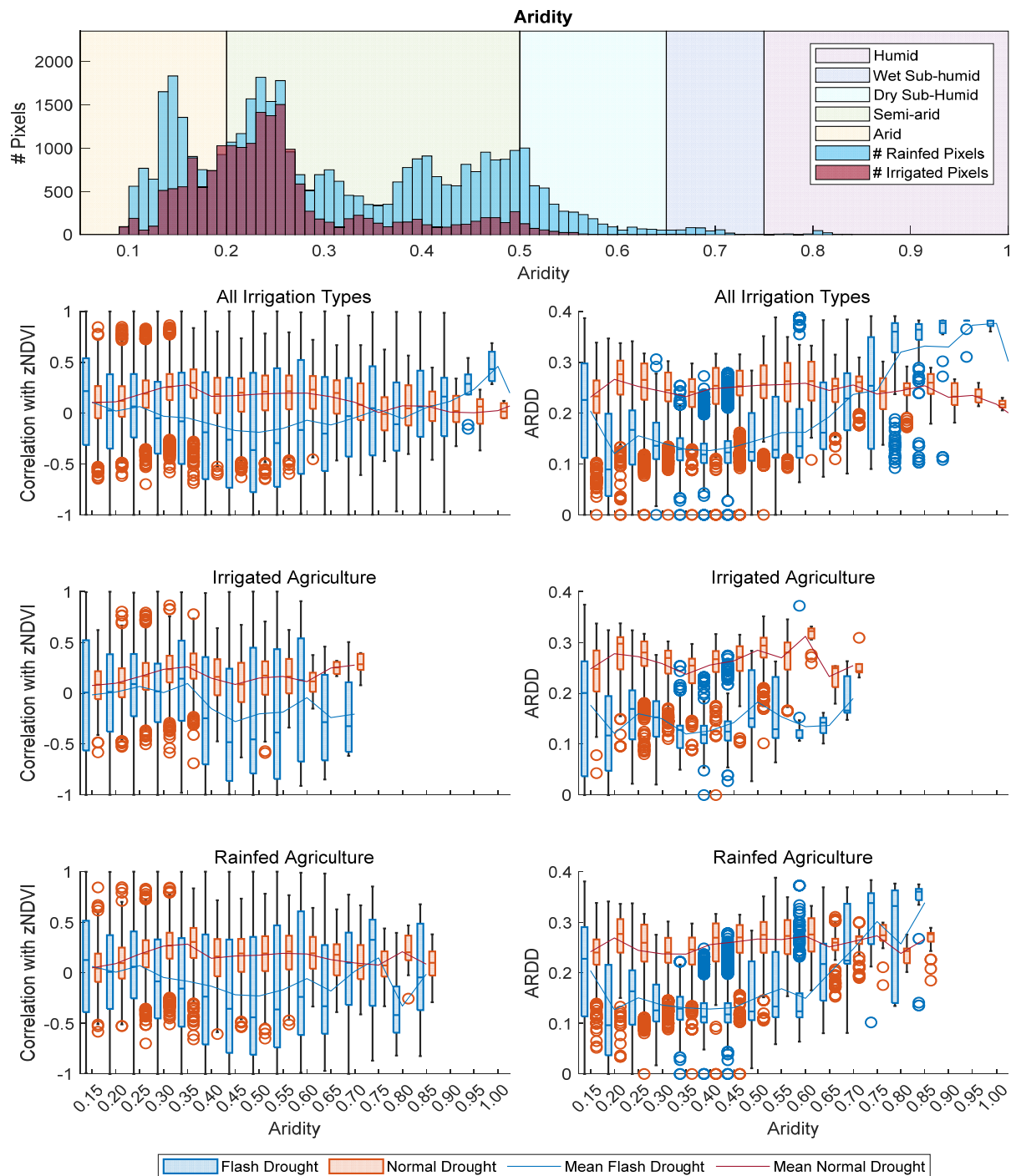
492 Figure 7. Density map illustrating the relationships between zNDVI-SSmI correlation and relative
493 duration for both drought types (normal, a & c; flash, b & d) and over different irrigation types (irrigated,
494 a & b; rainfed, c & d). Note the different color axes.

495 Density plots demonstrating the relationship between zNDVI-SSmI correlation with ARDD
496 (Figure 7) sought to answer H1. Normal drought (a & c) showed a generally decreasing average
497 correlation with increasing relative duration; however, the correlation remained overall positive
498 and rather densely compacted. This decrease is contradictory to the expectation (corollary to
499 H1): instead of worsening impacts with increased relative duration, pixels spending longer in
500 drought seem to exhibit a weaker correlation. A potential explanation could be that the longer
501 overall drought durations erode the relationship between SSmI and NDVI. Moderate drought
502 conditions, sustained over weeks, can cause deterioration in crops; if this has already occurred,
503 an increase in dryness would likely not cause further deterioration. Flash drought, on the other
504 hand, show correlations that are more frequently negative or close to zero, with considerable
505 noise outside of a few small hotspots (b & d). This noise could be due to the lag in response time
506 between soil moisture and vegetation condition (Otkin et al., 2016; C. Peng et al., 2014);
507 however, because the flash drought detection method accounts for a recovery period, this may
508 already be partially considered. Particularly interesting is the increased noise in irrigated flash
509 drought (b) over irrigated normal drought (a)—we hypothesize that this is the result of the
510 variety of irrigation techniques and crop types decoupling responses to drought by reducing the
511 deficit to varying degrees. Overall, while normal drought did indeed show more negative
512 consequences to vegetation than flash drought, longer relative duration within drought types did
513 not necessarily mean a more detrimental result to vegetation (H1).

514 4.4. Relationships of Characteristics to Aridity

515 Drought characteristics were analyzed with respect to aridity to further contextualize the
516 differences of flash and normal drought on agriculture, whether rainfed or irrigated. The aridity
517 is an expression of average available energy and water over a longer time period—previous
518 studies have indicated a relationship between aridity and vegetation response, with more arid
519 regions typically exhibiting a quicker and stronger response of vegetation to dry conditions.
520 (Orth et al., 2020; Vicente-Serrano et al., 2013). Many of the characteristics have shown
521 statistical differences between drought types and vegetation responses; however, the variable

522 spatial distribution of these characteristics imply a spatial reason for these differences. Because
 523 this variation seems to be aligned with the spatial distribution of aridity in the study region, the
 524 further investigation of characteristics of aridity in this section can help illustrate whether these
 525 statistical differences are due to geographic location and climate (which in this study area is
 526 related to aridity) or irrigation.



528 Figure 8. Relationships of relative duration and zNDVI-SSmI correlation to aridity.

529 4.4.1. Aridity and Relative Duration

530 ARDD in normal drought remains relatively stable throughout different aridity conditions and
531 exhibits similar patterns in both irrigation types (Figure 8). Because the dataset does not include
532 the effects of irrigation on soil moisture, this similar behavior is rather expected. The longest
533 relative durations for flash drought are associated with the highest aridity (most humid
534 conditions), where increased duration implies increased humidity. This behavior seems to be in
535 agreement with Orth et al. (2020), who found an increase in relative duration with increasing
536 dryness. While there is a slight increase in relative duration with increasing dryness, this trend is
537 not nearly as strong as that of increasing wetness. This strong relationship between relative
538 duration and humidity may be due to the average soil moisture anomaly in each region—due to
539 the larger deficit in humid regions, it may take longer for the volumetric soil moisture to return to
540 normal conditions. Thus, it can be hypothesized that the relative duration is more strongly related
541 to soil type than to aridity.

542 4.4.2. Aridity and Correlation to zNDVI

543 Normal drought for all irrigation types maintains a slightly positive correlation across all aridity
544 categories (Figure 8), with slight swelling in the semiarid region (~ 0.35) and slight decreases in
545 the wetter semi-arid and dry sub-humid regions demonstrating the impact of aridity (H2).
546 Overall, the irrigated regions have a weaker correlation, indicating that the added water does
547 indeed temper the potential adverse responses (H3). However, the relatively high correlations for
548 the most humid regions in irrigated areas indicates that the irrigation there may not be able to
549 compensate for the sustained deficits. This could potentially result from more water-intensive
550 crops being grown in this region that require more water than normal.

551 The low correlations for normal drought in the most arid regions seem to contradict Orth et al.
552 (2020)'s and Vicente-Serrano et al. (2013)'s findings that arid regions have quicker and stronger
553 responses to drought conditions (for both crops and forests). However, this could be due to the
554 fact that these studies focus on drought on longer time scales (months vs sub-monthly in this
555 study) and on larger regions (global studies vs this regional study). The shorter accumulation
556 periods used for SSmI and the drought detection method being optimized for flash drought may

557 result in events that are too sensitive to short-term changes in soil moisture and subsequently not
558 result in the higher deficits found in longer accumulation periods. It may also be due to the
559 diminishing difference in actual soil moisture indicated by a standardized value: as soil moisture
560 decreases, the difference in soil moisture to required to render more intense drought also
561 decreases. Thus, actual soil moisture deficits in arid regions may actually be quite small (Figure
562 6) and the vegetation grown there may be much more suited to adapting to the already-dry
563 conditions (H2).

564 Flash drought for all irrigation types shows slightly positive correlations in the arid and driest
565 semi-arid regions that become increasingly negative in the semi-arid and dry sub-humid regions
566 and increase drastically in the humid regions (H2). That the most positive correlations are in the
567 most arid and most humid regions agrees with Vicente-Serrano et al. (2013)'s findings that these
568 regions are most sensitive to drought conditions.. Overall, irrigated agriculture seems to be more
569 positively affected by flash drought, indicated by the steeper decrease in correlation between the
570 drier semi-arid and the wetter semi-arid regions than in rainfed agriculture. This seems to give
571 credence to Dong et al. (2019)'s hypothesis that this is a result of wetter regions having more
572 available sunlight and energy for photosynthesis, resulting in improved vegetation condition,
573 since irrigation bridges the water-energy gap and thus allows a speedier recovery from drought
574 conditions. However, when the environment becomes dry enough (aridity < 0.35), irrigation
575 loses its effectiveness on the vegetation condition (H3), resulting in more positive correlations
576 (for more, see S4).

577 **5 Conclusions**

578 This study has provided the following insights into the hypotheses outlined in the introduction:

- 579 • H1 – The results indicate that normal drought does indeed have more spatially
580 homogeneous drought characteristics (both ARDD and vegetation response expressed as
581 the correlation between zNDVI and SSml) and a more negative impact on vegetation
582 than flash drought. However, the corollary—that regions with a higher relative duration
583 within a drought type will experience stronger changes—does not seem to be true. The
584 relationship between ARDD and vegetation response seems to slightly decrease with
585 increasing relative duration in normal drought (potentially due to length of stress

586 decoupling the response), and shows little observable trend in flash drought aside from a
587 strong beneficial response at the highest relative duration.

- 588 • H2 – Signals of vegetation responses to increasing SSmI dryness show considerable
589 variation with aridity. As hypothesized, agriculture in humid regions does benefit from
590 flash drought events due to a lack of a true plant water deficit, which is dependent on soil
591 texture, and a short relative duration. Vegetation responses in hyperarid sections
592 experiencing normal drought also seem to show a more muted response than expected—
593 this may also be related to the actual deficit in soil moisture being quite small.
- 594 • H3 – Irrigation does indeed seem to temper adverse vegetation responses to both types of
595 drought; however, the impacts seem to differ depending on the aridity. Overall, irrigation
596 does reduce adverse vegetation response in normal drought aside from the exception of
597 wet sub-humid regions (which may simply be too sparsely populated to form a
598 representative sample). In flash drought, irrigated agriculture performs better than rainfed
599 in most aridity regimes; however, once the climate reaches a certain dryness, irrigation
600 seems to be less impactful.

601 This study is primarily limited by the available data: while the WLDAS dataset is the highest-
602 resolution and longest-running available in the region, it is still a reanalysis dataset and, despite
603 high performance in evapotranspiration and leaf-area-index measures, does not currently directly
604 include soil moisture observations or contributions from irrigation. This could affect drought
605 identification and relative duration information for irrigated areas. Moreover, the small number
606 of flash drought events analyzed in this study could have produced less robust results.

607 However, the elucidation of potential effects of flash drought in comparison to traditional
608 drought provided by this study may prove useful insights into impacts of flash drought,
609 particularly for agricultural regions. The analysis of vegetation condition in different aridity
610 regions during flash drought provides potentially generalizable insight into how the local climate
611 can impact vegetation responses to drought. The changing effect of irrigation on vegetation
612 during drought based on a location's aridity shows that, while it certainly can overcome negative
613 effects in some regions, it may not be as impactful as expected in others. This study has shown
614 that this could be due to the inability of standardized definitions to communicate or show deficits
615 that will actually hamper vegetation growth. Investigations of drought on vegetation should

616 therefore consider the actual available soil moisture and soil texture when drawing conclusions.
617 Such investigation, in the face of the distinctly different characteristics of flash and traditional
618 drought, may prove useful for preparing adaptation strategies in the future.

619 **Acknowledgments**

620 The authors would like to thank the editors and anonymous reviewers for their time and
621 insightful comments in reviewing this paper. The authors declare that they have no known
622 competing financial interests or personal relationships that could have appeared to influence the
623 work reported in this paper. The work is supported by the Technical University of Munich under
624 the framework of TUM Innovation Network “EarthCare” funded under the Excellence Strategy
625 of the Federal Government and the Länder.

626 **Open Research**

627 Soil moisture data and components to calculate potential ET (for aridity calculation) from
628 WLDAS used for drought identification and analysis in the study is available at NCCS
629 Dataportal (https://portal.nccs.nasa.gov/datashare/WLDAS/wldas_domain/). The DEM—also
630 used for potential ET calculation—is available through the USGS EarthExplorer
631 (<https://earthexplorer.usgs.gov/>; Data Sets > Digital Elevation > SRTM > SRTM 1 Arc-Second
632 Global). The crop mask used to identify irrigated and rainfed cropland (GFSAD1KCM) is
633 available through the LP DAAC (<https://lpdaac.usgs.gov/products/gfsad1kcmv001/>). Smoothed
634 and gap-filled MODIS NDVI data used for vegetation condition is available through ORNL
635 DAAC (<https://doi.org/10.3334/ORNLDAAC/1299>). Soil texture data is available through the
636 California Soil Resource Lab (<https://casoilresource.lawr.ucdavis.edu/soil-properties/>).

637

638 **References**

- 639 AghaKouchak, A. (2014). A baseline probabilistic drought forecasting framework using standardized soil moisture
640 index: application to the 2012 United States drought. *Hydrology and Earth System Sciences*, 18(7), 2485-
641 2492.
- 642 AghaKouchak, A., Farahmand, A., Melton, F. S., Teixeira, J., Anderson, M. C., Wardlow, B. D., & Hain, C. R.
643 (2015). Remote sensing of drought: Progress, challenges and opportunities. *Reviews of Geophysics*, 53(2),
644 452-480.
- 645 Bayissa, Y., Maskey, S., Tadesse, T., van Andel, S., Moges, S., van Griensven, A., & Solomatine, D. (2018).
646 Comparison of the Performance of Six Drought Indices in Characterizing Historical Drought for the Upper
647 Blue Nile Basin, Ethiopia. *Geosciences*, 8(3).

- 648 Buras, A., Rammig, A., & Zang, C. S. (2020). Quantifying impacts of the 2018 drought on European ecosystems in
649 comparison to 2003. *Biogeosciences*, 17(6), 1655-1672.
- 650 Chen, L. G., Gottschalck, J., Hartman, A., Miskus, D., Tinker, R., & Artusa, A. (2019). Flash Drought
651 Characteristics Based on U.S. Drought Monitor. *Atmosphere*, 10(9).
- 652 Cody, B. A., Folger, P., & Brougher, C. M. (2015). California drought: Hydrological and regulatory water supply
653 issues. In: Congressional Research Service Washington, DC.
- 654 Dong, C., MacDonald, G. M., Willis, K., Gillespie, T. W., Okin, G. S., & Williams, A. P. (2019). Vegetation
655 Responses to 2012–2016 Drought in Northern and Southern California. *Geophysical Research Letters*,
656 46(7), 3810-3821.
- 657 Erlingis, J. M., Rodell, M., Peters-Lidard, C. D., Li, B., Kumar, S. V., Famiglietti, J. S., et al. (2021). A High-
658 Resolution Land Data Assimilation System Optimized for the Western United States. *JAWRA Journal of*
659 *the American Water Resources Association*.
- 660 Farahmand, A., & AghaKouchak, A. (2015). A generalized framework for deriving nonparametric standardized
661 drought indicators. *Advances in Water Resources*, 76, 140-145.
662 <https://www.sciencedirect.com/science/article/abs/pii/S0309170814002322?via%3Dihub>
- 663 Ford, T. W., & Labosier, C. F. (2017). Meteorological conditions associated with the onset of flash drought in the
664 Eastern United States. *Agricultural and Forest Meteorology*, 247, 414-423.
- 665 Ford, T. W., McRoberts, D. B., Quiring, S. M., & Hall, R. E. (2015). On the utility of in situ soil moisture
666 observations for flash drought early warning in Oklahoma, USA. *Geophysical Research Letters*, 42(22),
667 9790-9798.
- 668 Gillespie, T. W., Ostermann-Kelm, S., Dong, C., Willis, K. S., Okin, G. S., & MacDonald, G. M. (2018).
669 Monitoring changes of NDVI in protected areas of southern California. *Ecological Indicators*, 88, 485-494.
- 670 Goldberg, A., Panov, N., Gutman, G. G., Imhoff, M. L., Anderson, M., Pinker, R. T., et al. (2010). Use of NDVI and
671 Land Surface Temperature for Drought Assessment: Merits and Limitations. *Journal of Climate*, 23(3),
672 618-633.
- 673 Griffin, D., & Anchukaitis, K. J. (2014). How unusual is the 2012-2014 California drought? *Geophysical Research*
674 *Letters*, 41(24), 9017-9023.
- 675 Griffith, G. E., Omernik, J. M., Smith, D. W., Cook, T. D., Tallyn, E., Moseley, K., & Johnson, C. B. (2016).
676 *Ecoregions of California* (2016-1021). Retrieved from Reston, VA:
677 <http://pubs.er.usgs.gov/publication/ofr20161021>
- 678 Gringorten, I. I. (1963). A plotting rule for extreme probability paper. *Journal of Geophysical Research*, 68(3), 813-
679 814.
- 680 Gu, Y., Brown, J. F., Verdin, J. P., & Wardlow, B. (2007). A five-year analysis of MODIS NDVI and NDWI for
681 grassland drought assessment over the central Great Plains of the United States. *Geophysical Research*
682 *Letters*, 34(6).
- 683 Guo, H., Bao, A., Liu, T., Jiapaer, G., Ndayisaba, F., Jiang, L., et al. (2018). Spatial and temporal characteristics of
684 droughts in Central Asia during 1966-2015. *Sci Total Environ*, 624, 1523-1538.
685 <https://www.ncbi.nlm.nih.gov/pubmed/29929262>
- 686 Guo, H., Bao, A., Ndayisaba, F., Liu, T., Jiapaer, G., El-Tantawi, A. M., & De Maeyer, P. (2018). Space-time
687 characterization of drought events and their impacts on vegetation in Central Asia. *Journal of Hydrology*,
688 564, 1165-1178.
- 689 Hao, Z., & AghaKouchak, A. (2013). Multivariate Standardized Drought Index: A parametric multi-index model.
690 *Advances in Water Resources*, 57, 12-18.
- 691 Ho, S. Q.-G., Tian, L., Disse, M., & Tuo, Y. (2021). A New Approach to Quantify Propagation Time from
692 Meteorological to Hydrological Drought. *Journal of Hydrology*, 127056.

- 693 Huang, S., Tang, L., Hupy, J. P., Wang, Y., & Shao, G. (2020). A commentary review on the use of normalized
694 difference vegetation index (NDVI) in the era of popular remote sensing. *Journal of Forestry Research*,
695 32(1), 1-6.
- 696 Ji, L., & Peters, A. J. (2003). Assessing vegetation response to drought in the northern Great Plains using vegetation
697 and drought indices. *Remote Sensing of Environment*, 87(1), 85-98.
- 698 Le Houerou, H. (1996). Climate change, drought and desertification. *Journal of Arid Environments*, 34.
- 699 Li, J., Wang, Z., Wu, X., Chen, J., Guo, S., & Zhang, Z. (2020). A new framework for tracking flash drought events
700 in space and time. *Catena*, 194.
- 701 Lisonbee, J., Woloszyn, M., & Skumanich, M. (2021). Making sense of flash drought: definitions, indicators, and
702 where we go from here. *Journal of Applied and Service Climatology*, 2021(1), 1-19.
- 703 Liu, Y., Zhu, Y., Ren, L., Otkin, J. A., Hunt, E. D., Yang, X., et al. (2020). Two Different Methods for Flash
704 Drought Identification: Comparison of Their Strengths and Limitations. *Journal of Hydrometeorology*,
705 21(4), 691-704.
- 706 Lloyd-Hughes, B. (2013). The impracticality of a universal drought definition. *Theoretical and Applied*
707 *Climatology*, 117(3-4), 607-611.
- 708 Lu, J., Carbone, G. J., Huang, X., Lackstrom, K., & Gao, P. (2020). Mapping the sensitivity of agriculture to drought
709 and estimating the effect of irrigation in the United States, 1950–2016. *Agricultural and Forest*
710 *Meteorology*, 292-293.
- 711 Lund, J., Medellin-Azuara, J., Durand, J., & Stone, K. (2018). Lessons from California's 2012–2016 Drought.
712 *Journal of Water Resources Planning and Management*, 144(10).
- 713 Marston, L., & Konar, M. (2017). Drought impacts to water footprints and virtual water transfers of the Central
714 Valley of California. *Water Resources Research*, 53(7), 5756-5773.
- 715 McKee, T. B., Doesken, N. J., & McKee, J. K. (1993). The relationship of drought frequency and duration to time
716 scales. *Eighth Conference on Applied Climatology*, 17.
- 717 Mo, K. C., & Lettenmaier, D. P. (2015). Heat wave flash droughts in decline. *Geophysical Research Letters*, 42(8),
718 2823-2829.
- 719 NASA-JPL. (2013). *NASA Shuttle Radar Topography Mission Global 1 arc second*.
- 720 Nguyen, H., Wheeler, M. C., Otkin, J. A., Cowan, T., Frost, A., & Stone, R. (2019). Using the evaporative stress
721 index to monitor flash drought in Australia. *Environmental Research Letters*, 14(6).
- 722 Nicolai-Shaw, N., Zscheischler, J., Hirschi, M., Gudmundsson, L., & Seneviratne, S. I. (2017). A drought event
723 composite analysis using satellite remote-sensing based soil moisture. *Remote Sensing of Environment*,
724 203, 216-225.
- 725 Okin, G. S., Dong, C., Willis, K. S., Gillespie, T. W., & MacDonald, G. M. (2018). The Impact of Drought on
726 Native Southern California Vegetation: Remote Sensing Analysis Using MODIS-Derived Time Series.
727 *Journal of Geophysical Research: Biogeosciences*, 123(6), 1927-1939.
- 728 Orth, R., & Destouni, G. (2018). Drought reduces blue-water fluxes more strongly than green-water fluxes in
729 Europe. *Nature Communications*, 9(1), 3602.
- 730 Orth, R., Destouni, G., Jung, M., & Reichstein, M. (2020). Large-scale biospheric drought response intensifies
731 linearly with drought duration in arid regions. *Biogeosciences*, 17(9), 2647-2656.
- 732 Otkin, J. A., Svoboda, M., Hunt, E. D., Ford, T. W., Anderson, M. C., Hain, C., & Basara, J. B. (2018). Flash
733 Droughts: A Review and Assessment of the Challenges Imposed by Rapid-Onset Droughts in the United
734 States. *Bulletin of the American Meteorological Society*, 99(5), 911-919.
- 735 Otkin, J. A., Zhong, Y., Hunt, E. D., Basara, J., Svoboda, M., Anderson, M. C., & Hain, C. (2016). Assessing the
736 evolution of soil moisture and vegetation conditions during a flash drought–flash recovery sequence over
737 the South-Central United States. *Journal of Hydrometeorology*, 20(3), 549-562.

- 738 Pauloo, R. A., Escriva-Bou, A., Dahlke, H., Fencl, A., Guillon, H., & Fogg, G. E. (2020). Domestic well
739 vulnerability to drought duration and unsustainable groundwater management in California's Central
740 Valley. *Environmental Research Letters*, 15(4).
- 741 Pendergrass, A. G., Meehl, G. A., Pulwarty, R., Hobbins, M., Hoell, A., AghaKouchak, A., et al. (2020). Flash
742 droughts present a new challenge for subseasonal-to-seasonal prediction. *Nature Climate Change*, 10(3),
743 191-199.
- 744 Peng, C., Deng, M., & Di, L. (2014). Relationships Between Remote-Sensing-Based Agricultural Drought
745 Indicators and Root Zone Soil Moisture: A Comparative Study of Iowa. *IEEE Journal of Selected Topics in
746 Applied Earth Observations and Remote Sensing*, 7(11), 4572-4580.
- 747 Peng, J., Dadson, S., Hirpa, F., Dyer, E., Lees, T., Miralles, D. G., et al. (2020). A pan-African high-resolution
748 drought index dataset. *Earth System Science Data*, 12(1), 753-769.
- 749 Peters, A. J., Walter-Shea, E. A., Ji, L., Vina, A., Hayes, M., & Svoboda, M. D. (2002). Drought monitoring with
750 NDVI-based standardized vegetation index. *Photogrammetric engineering and remote sensing*, 68(1), 71-
751 75.
- 752 Saxton, K. E., & Rawls, W. J. (2006). Soil Water Characteristic Estimates by Texture and Organic Matter for
753 Hydrologic Solutions. *Soil Science Society of America Journal*, 70(5), 1569-1578.
- 754 Sheffield, J., Andreadis, K. M., Wood, E. F., & Lettenmaier, D. P. (2009). Global and Continental Drought in the
755 Second Half of the Twentieth Century: Severity–Area–Duration Analysis and Temporal Variability of
756 Large-Scale Events. *Journal of Climate*, 22(8), 1962-1981.
- 757 Spinoni, J., Barbosa, P., De Jager, A., McCormick, N., Naumann, G., Vogt, J. V., et al. (2019). A new global
758 database of meteorological drought events from 1951 to 2016. *J Hydrol Reg Stud*, 22, 100593.
759 <https://www.ncbi.nlm.nih.gov/pubmed/32257820>
- 760 Spruce, J. P., Gasser, G. E., & Hargrove, W. W. (2016). MODIS NDVI Data, Smoothed and Gap-filled, for the
761 Conterminous US: 2000-2015. <http://dx.doi.org/10.3334/ORNLDAAAC/1299>
- 762 Stagge, J. H., Tallaksen, L. M., Gudmundsson, L., Van Loon, A. F., & Stahl, K. (2015). Candidate Distributions for
763 Climatological Drought Indices (SPI and SPEI). *International Journal of Climatology*, 35(13), 4027-4040.
- 764 Svoboda, M., LeComte, D., Hayes, M., Heim, R., Gleason, K., Angel, J., et al. (2002). The drought monitor. *Bulletin
765 of the American Meteorological Society*, 83(8), 1181-1190.
- 766 Taylor, R. (1990). Interpretation of the correlation coefficient: a basic review. *Journal of diagnostic medical
767 sonography*, 6(1), 35-39.
- 768 Teluguntla, P., Thenkabail, P., Xiong, J., Gumma, M., Giri, C., Milesi, C., et al. (2015). Global food security support
769 analysis data (GFSAD) at nominal 1 km (GCAD) derived from remote sensing in support of food security
770 in the twenty-first century: Current achievements and future possibilities.
- 771 Tucker, C. J. (1979). Red and photographic infrared linear combinations for monitoring vegetation. *Remote Sensing
772 of Environment*, 8(2), 127-150.
- 773 Vicente-Serrano, S. M., Gouveia, C., Camarero, J. J., Begueria, S., Trigo, R., Lopez-Moreno, J. I., et al. (2013).
774 Response of vegetation to drought time-scales across global land biomes. *Proc Natl Acad Sci U S A*,
775 110(1), 52-57. <https://www.ncbi.nlm.nih.gov/pubmed/23248309>
- 776 Vicente-Serrano, S. M., Miralles, D. G., Domínguez-Castro, F., Azorin-Molina, C., El Kenawy, A., McVicar, T. R.,
777 et al. (2018). Global Assessment of the Standardized Evapotranspiration Deficit Index (SEDI) for Drought
778 Analysis and Monitoring. *Journal of Climate*, 31(14), 5371-5393.
- 779 Walkinshaw, M., O'Geen, A. T., & Beaudette, D. E. (2022). Soil Properties. Retrieved from
780 casoilresource.lawr.ucdavis.edu/soil-properties/
- 781 Wang, L., & Yuan, X. (2018). Two Types of Flash Drought and Their Connections with Seasonal Drought.
782 *Advances in Atmospheric Sciences*, 35(12), 1478-1490.

- 783 Wilson, T. S., Sleeter, B. M., & Cameron, D. R. (2016). Future land-use related water demand in California.
784 *Environmental Research Letters*, 11(5).
- 785 Xiao, M., Koppa, A., Mekonnen, Z., Pagán, B. R., Zhan, S., Cao, Q., et al. (2017). How much groundwater did
786 California's Central Valley lose during the 2012-2016 drought? *Geophysical Research Letters*, 44(10),
787 4872-4879.
- 788 Xiao, X., Flanagan, P. X., Wakefield, R. A., Hunt, E. D., Otkin, J. A., Basara, J. B., & Christian, J. I. (2019). A
789 Methodology for Flash Drought Identification: Application of Flash Drought Frequency across the United
790 States. *Journal of Hydrometeorology*, 20(5), 833-846.
- 791 Xue, J., & Su, B. (2017). Significant Remote Sensing Vegetation Indices: A Review of Developments and
792 Applications. *Journal of Sensors*, 2017, 1-17. review.
- 793 Zang, C. S., Buras, A., Esquivel-Muelbert, A., Jump, A. S., Rigling, A., & Rammig, A. (2019). Standardized
794 drought indices in ecological research: Why one size does not fit all. *Glob Chang Biol*, 26(2), 322-324.
795 <https://www.ncbi.nlm.nih.gov/pubmed/31442346>
- 796 Zomer, R. J., & Trabucco, A. (2022). Global Aridity Index and Potential Evapo-Transpiration Dataset v3. In.
- 797 Zotarelli, L., Dukes, M. D., Romero, C. C., Migliaccio, K. W., & Morgan, K. T. (2010). Step by step calculation of
798 the Penman-Monteith Evapotranspiration (FAO-56 Method). *Institute of Food and Agricultural Sciences*.
799 *University of Florida*.
- 800
- 801